Journal of Inflammation Research

Dovepress
Taylor & Francis Group

Open Access Full Text Article

ORIGINAL RESEARCH

# Downregulated RSAD2 Attenuates the Apoptosis of LPS-Stimulated RAW264.7 via NF-κB Signaling Pathway

Zhen Qi[1,2,*], Kongli Lu[1,*], Mengxi Huang[3], Haixia Wang[4], Rongheng Liao[1,5], Ri Tang[4]

[1]Department of Cardiovascular Surgery, Renji Hospital, School of Medicine, Shanghai Jiao Tong University, Shanghai, People's Republic of China; [2]Department of Cardiovascular Surgery, The Second Xiangya Hospital, Central South University, Changsha, People's Republic of China; [3]Jinshan Hospital, Fudan University, Shanghai, People's Republic of China; [4]Department of Critical Care Medicine, Renji Hospital, School of Medicine, Shanghai Jiao Tong University, Shanghai, People's Republic of China; [5]Department of Cardiology, Erasmus Medical Center, Rotterdam, 3015GD, The Netherlands

*These authors contributed equally to this work

Correspondence: Ri Tang; Rongheng Liao, Email raytong7@163.com; ronanliao@163.com



**Background:** This study aimed to investigate the role of Radical S-adenosyl Methionine Domain-Containing 2 (RSAD2) in regulating the apoptosis of LPS-stimulated RAW264.7 macrophages via the NF-κB signaling pathway.

**Methods:** Differentially expressed genes in LPS-stimulated macrophages were identified using a gene expression dataset from the Gene Expression Omnibus (GEO) database and analyzed with R software. Kyoto Encyclopedia of Genes and Genomes (KEGG) and Gene Ontology (GO) analyses were performed to predict the biological functions of the identified genes. Key genes involved in NF-κB-mediated apoptosis regulation were selected for further investigation. The expression levels of Bcl-2, cleaved caspase-3, and NF-κB p65 were assessed by Western blotting. TUNEL staining was used to evaluate apoptosis.

**Results:** RSAD2 knockdown significantly improved cell viability and reduced apoptosis in LPS-stimulated RAW264.7 cells. Downregulation of RSAD2 increased Bcl-2 expression and inhibited cleaved caspase-3 activity, thus inhibiting apoptosis. Mechanistically, the downregulation of RSAD2 suppressed the NF-κB signaling pathway in vitro. Treatment with phorbol 12-myristate 13-acetate (PMA), an NF-κB agonist, reversed the protective effects of RSAD2 knockdown in LPS-stimulated RAW264.7 cells.

**Conclusion:** Our findings suggested that RSAD2 knockdown alleviated LPS-induced apoptosis in RAW264.7 macrophages by suppressing the NF-κB signaling pathway, highlighting RSAD2 as a potential therapeutic target for sepsis-related macrophage dysfunction.

**Keywords:** sepsis, apoptosis, NF-κB pathway, RAW264.7, lipopolysaccharide

## Introduction

Sepsis is a clinical syndrome characterized by infection-induced dysregulation of the host immune response, ultimately leading to multiple organ dysfunction syndrome (MODS).[1] Among the affected organs, the lung is particularly susceptible and plays a critical role in the progression of the condition. Notably, over half of sepsis patients develop acute respiratory distress syndrome (ARDS) or acute lung injury (ALI).[2] Despite increasing research efforts in sepsis, effective therapeutic options beyond standardized treatments and supportive care remain limited.[3] Consequently, a deeper understanding of the biological processes underlying sepsis pathogenesis is essential for improving patient outcomes and advancing therapeutic strategies.

Macrophages, as essential components of the mononuclear phagocyte system, are widely distributed across tissues and perform diverse functions, including efferocytosis, phagocytosis, antibacterial defense, regulation of inflammation, vascular homeostasis, and erythropoiesis.[4,5] Among these, alveolar macrophages (AMs) are the predominant immune cells in lung tissue. By releasing excessive proinflammatory cytokines, AMs contribute to neutrophil infiltration and lung tissue damage, playing a pivotal role in sepsis progression.[2] This regulatory role of macrophages is closely tied to their

Received: 23 May 2025
Accepted: 7 August 2025
Published: 12 August 2025

polarization into distinct phenotypes: classically activated, proinflammatory macrophages (M1), and alternatively activated, anti-inflammatory/repair macrophages (M2).[6] M2 macrophages not only secrete anti-inflammatory cytokines but also facilitate the phagocytosis of apoptotic neutrophils, thereby mitigating inflammatory lung injury.[5]

In the early stages of sepsis, proinflammatory factors such as interferon-γ (IFN-γ) and lipopolysaccharide (LPS) drive proinflammatory macrophage polarization (M1).[6] LPS, a key endotoxin component of gram-negative bacterial cell walls, activates macrophages via the nuclear factor (NF)-κB signaling pathway, leading to the production of proinflammatory mediators such as nitric oxide (NO), IL-1, TNF-α, and IL-6.[7,8] These mediators, in turn, can activate the caspase cascade, ultimately inducing apoptosis in various cell types, including macrophages.[9] Additionally, recent studies have highlighted that inhibiting macrophage ferroptosis, a regulated form of cell death, can ameliorate sepsis-induced acute lung injury.[10] In sepsis patients, macrophage apoptosis is markedly elevated,[11] underscoring the critical importance of preventing excessive macrophage apoptosis in improving outcomes and alleviating tissue damage.

RSAD2, also known as Viperin, is an interferon-induced protein that is usually expressed at lower levels in ordinary cells but is significantly upregulated in cells after stimulation by type I interferons, various viruses, LPS, and poly (I:C).[12] RSAD2 is a highly conserved protein that can exert antiviral effects through various mechanisms, the most important of which is to generate 3′-deoxy-3′,4′-dihydrocytidine triphosphate (ddhCTP), which acts as a chain terminator, inhibits RNA polymerase and enhances innate immunity by regulating lipid synthesis and soluble protein secretion.[13] In addition to its antiviral role, RSAD2 has been implicated in tumor progression, where it facilitates metabolic reprogramming to support malignancy.[14] Additionally, studies have reported that RSAD2 promotes the development of psoriasis in keratinocytes by activating the TAK1-mediated NF-κB signaling pathway.[15] Furthermore, knockdown of RSAD2 suppresses the activation of the TLR2/MyD88/NF-κB signaling pathway in activated microglia.[16] These findings collectively suggest a potential regulatory relationship between RSAD2 and NF-κB. However, to the best of our knowledge, the effects and molecular mechanisms of RSAD2 in sepsis remain unexplored.

Here, we elucidated the pivotal role of RSAD2 knockout in mitigating apoptosis by directly modulating the NF-κB signaling pathway. Collectively, these findings indicated that RSAD2 is a potential therapeutic target for sepsis.

# Materials and Methods

## Regent

LPS (L2880) was obtained from Sigma (United States). Phorbol myristate acetate (PMA, S8877, ≥99.80% purity) was purchased from MCE Company (United States).

## Cell Culture and Treatment

The RAW264.7 cell line has been widely utilized in studies investigating macrophage functions, underlying mechanisms, and signal transduction pathways.[17] RAW264.7 macrophages were obtained from Cell Bank, Chinese Academy of Sciences (Shanghai) and cultured in DMEM medium, supplemented with 10% fetal bovine serum (FBS) at 37°C in a 5% CO2 incubator. LPS (1 μg/mL) was used to stimulate RAW264.7 cells for 24 hours. When the RAW264.7 cells reached approximately 70% confluency, a negative control (NC) and si-RSAD2 were transfected into the cells at a concentration of 30 pmol using Lipofectamine™ 3000 (Thermo, United States) for 48 hours before the next experiment. The detailed sequences are provided in Supplementary Table S1.

## RNA Extraction and Quantitative Real-Time PCR Analysis

An EZ-press RNA Purification Kit (EZbioscience, United States) was used to extract total cell RNA. The concentration and purity of the extracted RNA were determined via an ultra-micro ultraviolet spectrophotometer. Reverse transcription was carried out using PrimeScript™ RT reagent Kit (Takara, Japan). Twelve selected mRNAs were detected via real-time PCR in a LightCycler 480 system (Roche, Swiss) using TB Green® Premix Ex Taq™ Kit (Takara, Japan). The relative expression levels of the target genes were calculated via the $2^{-\Delta\Delta CT}$ method, with each sample being run in triplicate independently. The primers used are listed in Supplementary Table S2.

## Western Blot

Total protein was extracted via RIPA lysis buffer (Beyotime, China). The concentrations of these proteins were detected via a BCA Protein Assay kit (Thermo, USA). The proteins were then separated via sodium dodecyl sulfate–polyacrylamide gel electrophoresis (SDS–PAGE) and transferred to PVDF membranes. The PVDF membranes were blocked for 15 minutes at room temperature with protein-free rapid-blocking solution (Epizyme Biotech, China). The samples were subsequently incubated overnight at 4°C with antibodies against p-p65 (1:1000, Cell Signaling Technology, USA), RSAD2 (1:1000, Abcam, UK), cleaved caspase-3 (1:1000, Cell Signaling Technology, USA), Bcl-2 (1:1000, Abcam, UK), and GAPDH (1:1000, Abcam, UK). After three washes with TBST, the cells were incubated for 1 hour at room temperature with secondary antibodies. Another three washes with TBST were performed before the PVDF membrane was treated with an ECL chemiluminescence kit (Vazyme, China). The proteins were visualized via a chemiluminescence imager (Bio-Rad, UK). ImageJ software was used to analyze the gray values of the images.

## TUNEL Staining

The level of DNA damage was measured using a TUNEL kit (Beyotime, China). The cells in each group were fixed at room temperature with 4% polyformaldehyde for 20 min, washed with PBS 3 times, and then incubated with Immunostaining Permeabilization Solution (Beyotime, China) for 10 min. After washing with PBS 3 times, the TUNEL reagent was used to incubate the cells at 37°C for 2 h, and the cells were then sealed with Antifade Mounting Medium with DAPI (Beyotime, China). Finally, the TUNEL-positive cells were observed under a fluorescence microscope.

## Flow Cytometry

An Annexin V-FITC Apoptosis Detection Kit (BD, USA) was used. The cells in each group were collected, resuspended in precooled PBS, centrifuged, and discarded. Then, 300 μL of 1× binding buffer was added for resuspension, and 5 μL of Annexin V-FITC was added and mixed well. The mixture was protected from light and incubated at room temperature for 15 minutes. 5μL of PI was added for staining before loading, and 200 μL of 1×binding buffer was added. Analyze using FACS LSRFortessa X20 (BD, USA).

## MitoSOX™ Mitochondrial Superoxide Staining

According to the manufacturer's protocol of MitoSOX™ Red superoxide indicator (Invitrogen detection technologies, USA), prepare a 5 μM working solution by diluting the MitoSOX Red dye in serum-free medium. Remove the cell culture medium and gently wash the cells once with phosphate-buffered saline (PBS). The prepared MitoSOX Red working solution was added to the cells, which were subsequently incubated at 37°C in the dark for 10 minutes. After incubation, the cells were washed three times with PBS to remove excess dye. The fluorescence images were captured via an inverted fluorescence microscope. Semiquantitative analysis of the fluorescence intensity was performed via ImageJ software.

## JC-1 Staining

According to the manufacturer's instructions of the Mitochondrial Membrane Potential Assay Kit with JC-1 (Beyotime Biotechnology, China), the JC-1 staining working solution and JC-1 staining buffer were prepared. Following removal of the culture medium, 500 μL of fresh culture medium and 500 μL of JC-1 staining working solution were added to each well of the 12-well plate, followed by thorough mixing. The cells were then incubated at 37°C in the dark for 20 minutes. After incubation, the supernatant was removed, and the cells were washed twice with JC-1 staining buffer. Fluorescence images were captured via an inverted fluorescence microscope, and semiquantitative analysis was performed via ImageJ software.

## Cell Immunofluorescence Staining

The culture medium was removed, and the cells were gently washed twice with PBS. Then, 4% paraformaldehyde was added, and the cells were fixed at room temperature for 30 minutes. After fixation, the cells were washed three times with PBS for 5 minutes each. 0.1% Triton X-100 (dissolved in PBS) was added, and the samples were incubated at room

temperature for 10 minutes. Then, the cells were washed three times with PBS for 5 minutes each. Blocking buffer (5% BSA) was added, and the samples were incubated at room temperature for 1 hour. The blocking solution was removed, anti-p-p65 (1:250, Cell Signaling Technology, USA) was added, and the samples were incubated at 4°C overnight. After incubation, the cells were washed three times with PBS for 5 minutes each. Goat anti-rabbit IgG H&L (Alexa Fluor® 488; 1:200; Abcam; UK) was added, and incubated at room temperature in the dark for 1 hour. After incubation, the cells were washed three times with PBS for 5 minutes each. The coverslips were removed from the plate, Antifade Mounting Medium with DAPI was added, and the slides were sealed for storage in the dark. Fluorescence images were captured via a fluorescence microscope, and semiquantitative analysis was performed via ImageJ software.

## Bioinformatics Analysis

These mRNA sequencing data (GSE40885, species: *Homo sapiens*) were obtained from GENE EXPRESSION OMNIBUS (GEO) database. All samples were detected/re-identified by [HG-U133_Plus_2] Affymetrix Human Genome U133 Plus 2.0 Array. The mRNA data standardization and differential expression analysis (DEGs) were carried out by the DESeq R package (version 1.42.1). DEGs were identified via a cutoff of $|\log2(\text{fold change})| \geq 1$ and a $p$ value $<0.05$. Analysis of the sequencing data, including heatmap analysis, gene ontology (GO) analysis, Kyoto Encyclopedia of Genes and Genomes (KEGG), and Gene Set Enrichment Analysis (GSEA), was conducted using the Pheatmap R package (version 1.0.12) and clusterProfiler R package (version 4.10.1), respectively.

## Statistical Analysis

Data with normal distribution are presented as mean ± SD. Intergroup differences were assessed using Student's *t*-test for two-group comparisons and one-way ANOVA with Tukey's post hoc test for multiple groups. All statistical analyses were performed using GraphPad Prism 9.3. $p < 0.05$ was considered statistically significant.

# Results

## RSAD2 expression Was Upregulated in LPS-Induced RAW264.7 Cells

To identify novel biomarkers that serve as diagnostic indicators of sepsis and screen out the differentially expressed genes (DEGs), we analyzed the GSE40885 dataset of the GEO database. To assess the quality and distribution of the gene expression data, box plots were generated for all the samples from the GEO dataset. As shown in Supplementary Figure S1A, normalization of the raw expression data led to more consistent distributions across samples, enhancing data quality and ensuring its suitability for downstream analyses. Principal component analysis (PCA) showed the gene expression profiles between the Saline and LPS groups (Figure 1A). A representative heatmap revealed significant differences between the Saline and LPS groups (Figure 1B). To identify the most significant genes in the process of sepsis, volcano plots were constructed with a significance threshold of $p < 0.05$ and a fold change of $|\log FC| \geq 1$. The results revealed a total of 530 DEGs between macrophages stimulated with LPS and unstimulated macrophages, of which 470 were upregulated and 60 were downregulated (Figure 1C). To validate the bioinformatics analysis results, RAW264.7 cells were stimulated with LPS, and the genes with the most significant logFC differences identified in the sequencing data were selected for qPCR validation. As shown in Figure 1D, among the 12 genes analyzed, 6 were significantly downregulated (*TNFSF10, IFIT2, GPR183, GNG2, DDX58, and USP18*), 3 were significantly upregulated (*RSAD2, ATF3, and GBP5*), and 3 showed no significant changes (*ISG20, FPR2, and IFITM1*). Among these genes, *RSAD2* exhibited the most significant change and was closely associated with cell apoptosis and inflammation. Western blot showed that the protein expression level of RSAD2 was significantly upregulated in the LPS-induced RAW264.7 cells (Figure 1E and F). These results suggested that RSAD2 was a potential target of apoptosis in LPS-induced macrophages.

## The Mitochondrial Pathway of Apoptosis Is Activated in LPS-Induced RAW264.7 Cells

The pathology of sepsis involves multiple cell death pathways. In this study, we evaluated the expression of apoptosis-associated proteins using Western blot analysis. As shown in Figure 2A and B, the expression of the pro-apoptotic protein

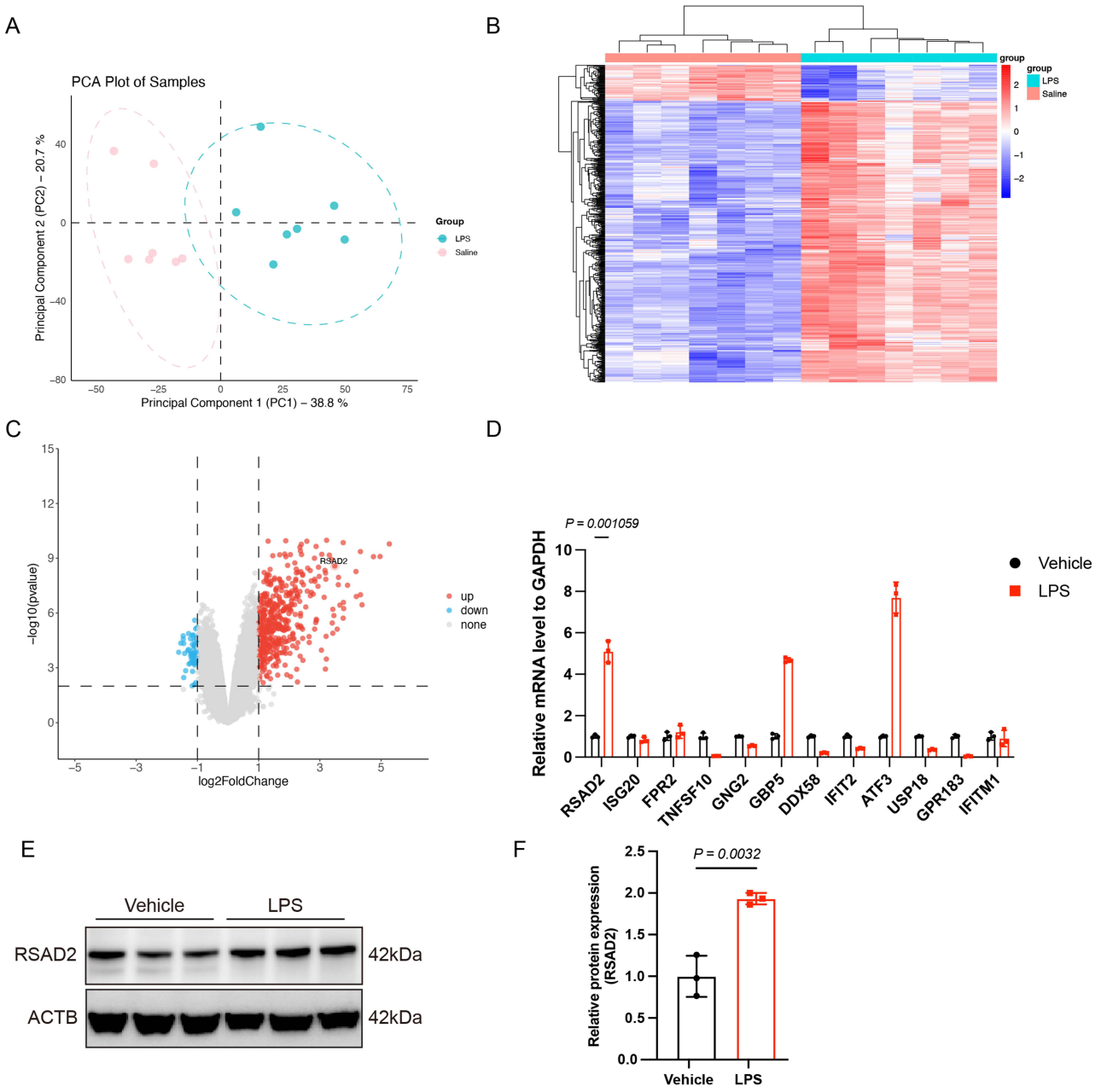


**Figure 1** RSAD2 expression was upregulated in LPS-induced RAW264.7 cells. (**A**) Principal component analysis (PCA) was used to distinguish the gene expression patterns between the Saline and LPS treatment groups. (**B**) Heatmap of differentially expressed genes (DEGs) in the LPS group compared to the Saline group, |log2(fold change) | ≥ 1, *p* value < 0.05. (**C**) Volcano map of DEGs. (**D**) The mRNA levels of the 12 DEGs (*RSAD2, ISG20, FPR2, TNFSF10, GNG2, GBP5, DDX58, IFIT2, ATF3, USP18, GPR183, and IFITM1*) were measured by qPCR. (**E**) The protein expression levels of RSAD2 were measured by Western Blot. (**F**) Semi-quantitative grayscale intensity analysis, n = 3. Data with normal distribution are presented as mean ± SD.

cleaved caspase-3 was significantly elevated in LPS-treated RAW264.7 cells, while the expression of the anti-apoptotic protein Bcl-2 was markedly reduced. TUNEL staining revealed a significant increase in the proportion of TUNEL-positive cells in LPS-treated RAW264.7 cells (Figure 2C and D). Similarly, mitoSOX staining indicated that LPS treatment promoted mitochondrial superoxide production (Figure 2E and F). Furthermore, JC-1 staining demonstrated a significant reduction in mitochondrial membrane potential (MMP) in LPS-treated RAW264.7 cells (Figure 2G and H). Collectively, these findings highlighted that LPS induced mitochondrial pathway-mediated apoptosis in RAW264.7 cells.


https://doi.org/10.2147/JIR.S535225

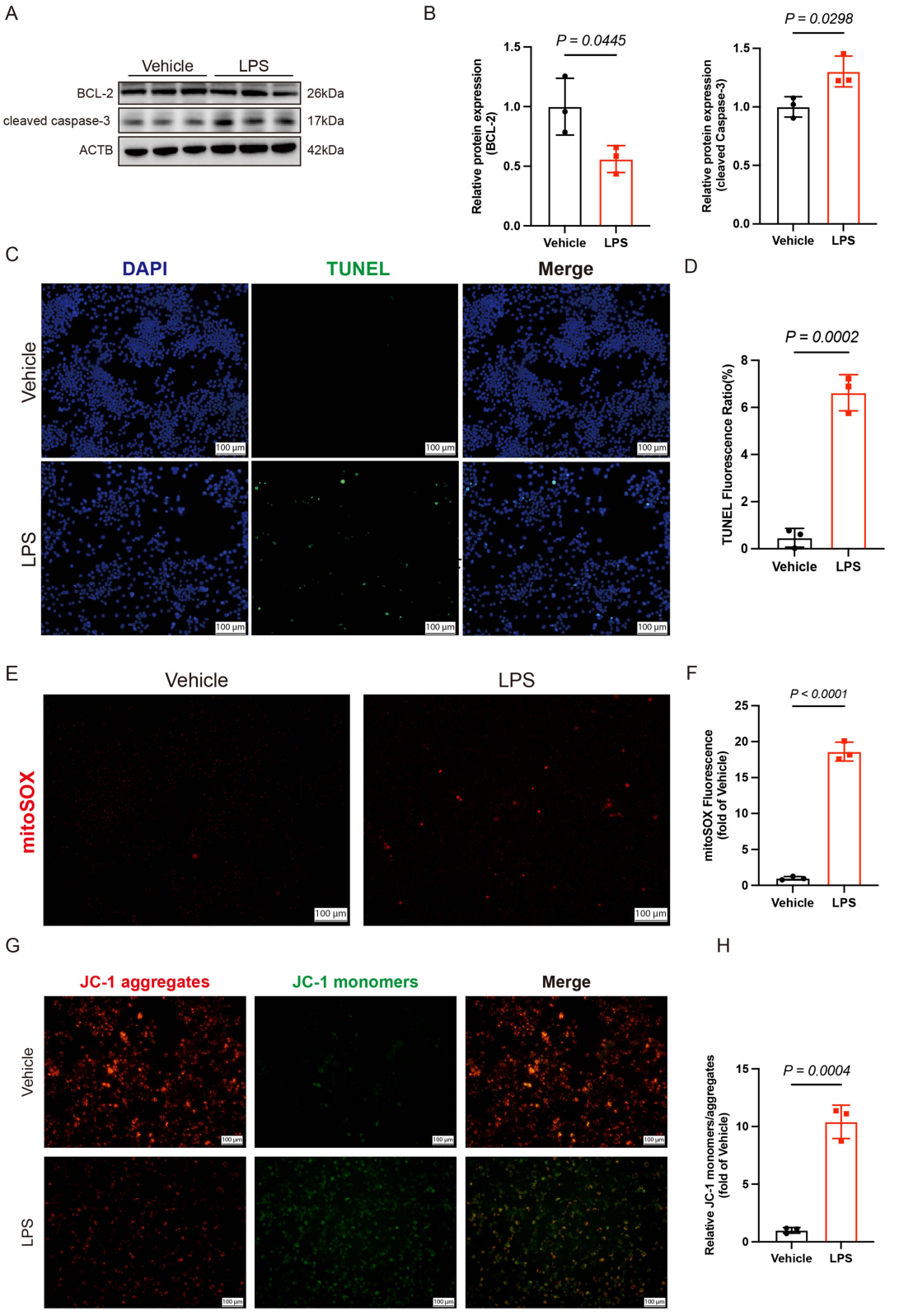


**Figure 2** The mitochondrial pathway of apoptosis is activated in LPS-induced RAW264.7 cells. (**A** and **B**) Western blot analysis and densitometric quantification of the protein expression levels of cleaved caspase-3 and Bcl-2, n = 3. (**C**) Apoptotic cells were identified by TUNEL-positive green fluorescence, while nuclei were counterstained with DAPI (blue). (**D**) Measurement of TUNEL-positive cell ratio, n = 3. (**E**) MitoSOX staining of RAW264.7. (**F**) Fluorescence intensity quantification of mitoSOX-positive cells, n = 3. (**G**) Typical JC-1 staining patterns observed in LPS-stimulated RAW264.7 cells. (**H**) Fluorescence signal intensity was quantified, n = 3. Data with normal distribution are presented as mean ± SD.

## RSAD2 Knockdown Attenuated Apoptosis in LPS-Induced RAW264.7 Cells

To investigate the role of RSAD2 in LPS-induced macrophage apoptosis, siRNA (siRSAD2) was used to knock down RSAD2 expression. Immunoblot analysis showed that siRSAD2 significantly inhibited the expression of RSAD2 (Supplementary Figure S1D). Subsequently, we assessed the impact of siRSAD2 on apoptosis in LPS-stimulated RAW264.7 cells. According to Western blot results, LPS treatment increased cleaved caspase-3 levels but reduced Bcl-2 expression. However, in LPS-induced RAW264.7 cells, siRSAD2 increased Bcl-2 protein levels and reduced cleaved caspase-3 expression. (Figure 3A and B). The TUNEL assay demonstrated that siRSAD2 treatment led to a significant reduction in TUNEL-positive RAW264.7 cells exposed to LPS. (Figure 3C and D). Meanwhile, siRSAD2 inhibited mitochondrial superoxide production (Figure 3E and F) and improved the mitochondrial membrane potential (Figure 3G and H) in LPS-induced RAW264.7 cells. These findings demonstrated that RSAD2 knockdown attenuated the apoptosis of LPS-induced RAW264.7 cells.

## Functional and Pathway Enrichment of DEGs

To further clarify the molecular mechanism underlying RSAD2-mediated regulation of macrophage apoptosis, we conducted GO and KEGG pathway enrichment analyses on the differentially expressed genes (DEGs) of GSE40885 dataset. GO analysis revealed that the DEGs were enriched primarily on the external side of the plasma membrane and specific granules at the cellular component (CC) level. At the biological process (BP) level, the DEGs were predominantly associated with the positive regulation of cytokine production and the response to lipopolysaccharide. At the molecular function (MF) level, the DEGs were mainly involved in cytokine receptor binding, cytokine activity, and G protein-coupled receptor binding (Figure 4A–C). KEGG pathway enrichment analysis revealed significant enrichment in pathways such as cytokine–cytokine receptor interaction, the NF–kappa B signaling pathway, and the NOD–like receptor signaling pathway (Figure 4D). To further explore the biological significance of the DEGs, gene set enrichment analysis (GSEA) was conducted. The results indicated significant upregulation of the apoptosis, inflammatory response, and the Nod1 2 signaling pathway (Figure 4E and F, S1B). Hub gene analysis reveals core regulatory genes such as RSAD2, NF-κB, and TNF (Supplementary Figure S1C). These results demonstrated that the NF-κB signaling pathway played a vital role in the LPS-induced RAW264.7 cell apoptosis.

## RSAD2 Knockdown Inhibited the Activation of NF-κB Signaling Pathway in vitro

To clarify whether the downregulation of RSAD2 inhibits the NF-κB signaling pathway in RAW264.7 cells, the expression of p-p65 was detected by Western blot. The results revealed that p-p65 was significantly activated in LPS-induced macrophages, whereas RSAD2 knockdown markedly suppressed the activation of the NF-κB signaling axis (Figure 5A and B). Immunofluorescence staining results showed that p-p65 was activated in LPS-induced RAW264.7 cells, accompanied by significant nuclear translocation (Figure 5C). ELISA data indicated concordant trends between NF-κB activity and its downstream cytokines (IL-6/TNF-α) (Supplementary Figure S1E and F). These results demonstrated that RSAD2 knockdown inhibited the activation of the NF-κB signaling pathway in vitro.

## PMA Reversed the Protective Effect of RSAD2 Knockdown on Apoptosis in vitro

To determine whether RSAD2 mitigates LPS-induced apoptosis in RAW264.7 cells via the NF-κB signaling pathway, phorbol 12-myristate 13-acetate (PMA), an activator of the NF-κB signaling pathway, was utilized to evaluate whether the anti-apoptotic effect resulting from RSAD2 downregulation could be reversed. Western blot and flow cytometry analyses demonstrated that PMA significantly activated the NF-κB signaling pathway and promoted the apoptosis of RAW264.7 cells. Knockdown of RSAD2 effectively inhibited LPS-induced activation of p65 and subsequent apoptosis. However, the protective effect of RSAD2 knockdown was reversed upon PMA treatment (Figure 6A and B and Figure 6I and J). TUNEL staining showed that the ratio of TUNEL-positive cells in the LPS + siRSAD2 + PMA group was markedly greater than that in the LPS + siRSAD2 group (Figure 6C and D). Meanwhile, PMA treatment reversed the inhibitory effect of RSAD2 knockdown on mitochondrial superoxide production (Figure 6E and F) as well as the

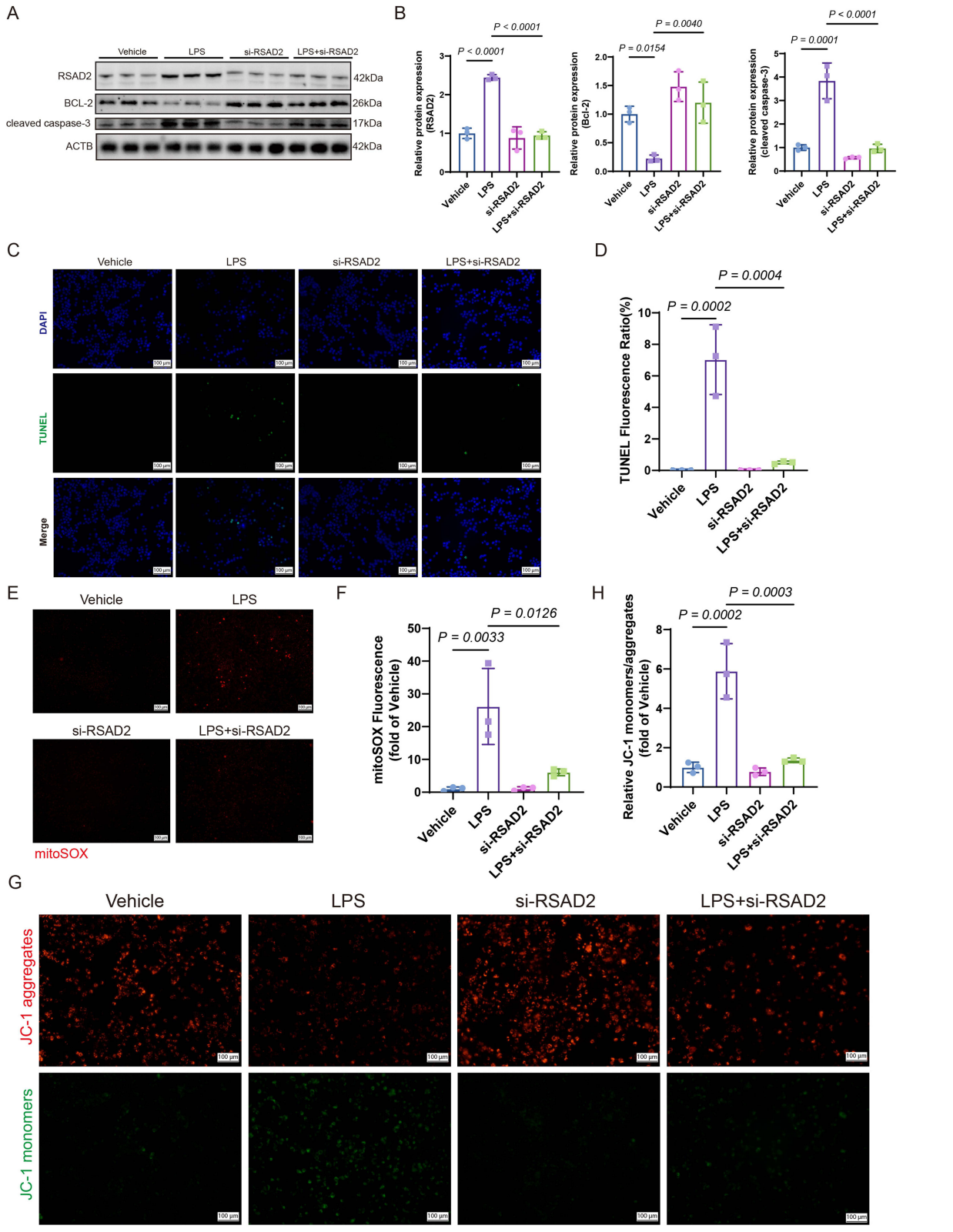


**Figure 3** RSAD2 knockdown attenuated apoptosis in LPS-induced RAW264.7 cells. (**A**) Western blot analysis of the protein expression levels of cleaved caspase-3 and Bcl-2. (**B**) Semi-quantitative grayscale intensity analysis, n = 3. (**C**) TUNEL staining of cell apoptosis. (**D**) Measurement of TUNEL-positive cell ratio, n = 3. (**E** and **F**) MitoSOX staining and fluorescence intensity quantification of RAW264.7, n = 3. (**G**) Typical JC-1 staining patterns observed in LPS-stimulated RAW264.7 cells. (**H**) Fluorescence signal intensity was quantified, n = 3. Data with normal distribution are presented as mean ± SD.

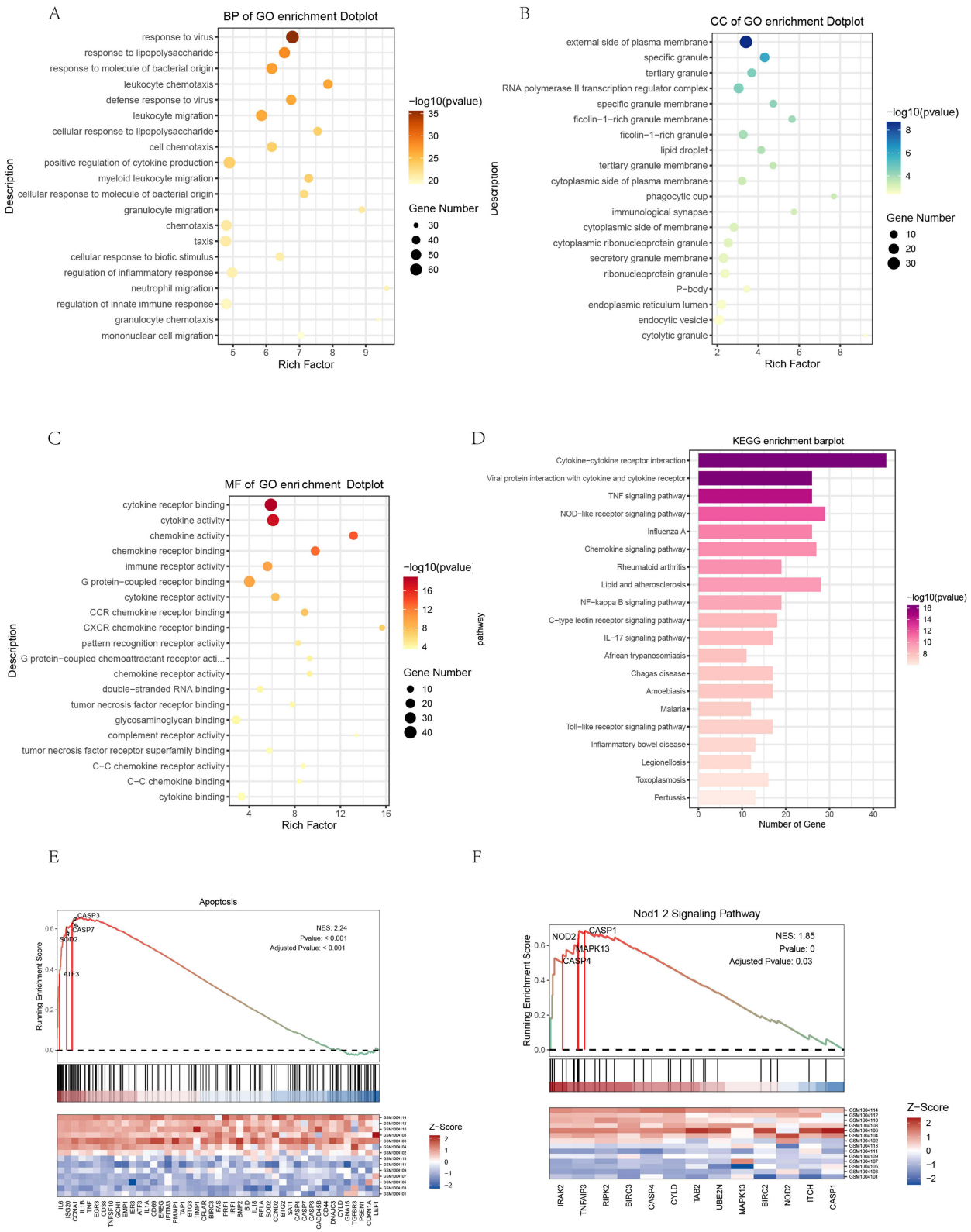


**Figure 4** Functional and pathway enrichment of DEGs. (**A**–**C**) Functional enrichment of DEGs in BP, CC, and MF of GO (**D**) The KEGG analysis enriched the top 10 significant pathways of DEGs. (**E** and **F**) GSEA analysis of the differentially expressed genes.


https://doi.org/10.2147/JIR.S535225

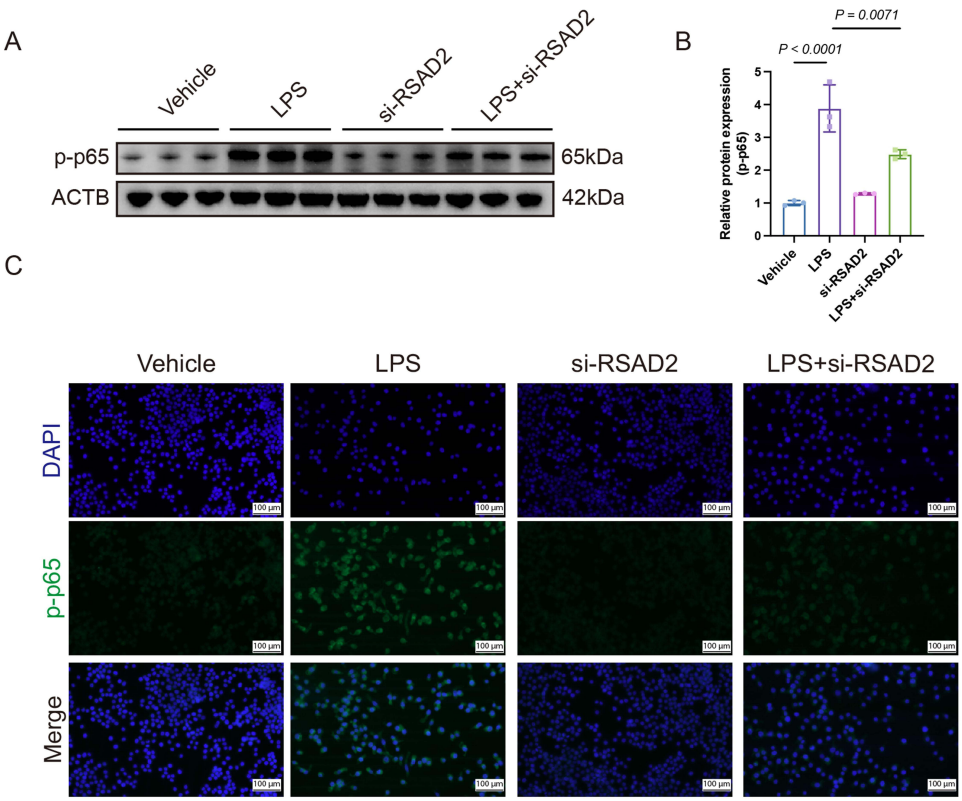


**Figure 5** RSAD2 knockdown inhibited the activation of NF-kB signaling pathway in vitro. (**A**) Western blot analysis of the protein expression levels of p-p65. (**B**) Semi-quantitative grayscale intensity analysis, n = 3. (**C**) Representative immunofluorescence staining for p-p65. Data with normal distribution are presented as mean ± SD.

protective effect on mitochondrial membrane potential (Figure 6G and H). These findings indicated that PMA counteracted the anti-apoptotic effects of RSAD2 silencing in RAW264.7 cells.

## Discussion

In the present study, we found an increase in RSAD2 levels in human alveolar macrophages exposed to LPS and in RAW264.7 cells. Loss-of-function experiments revealed that RSAD2 plays a protective role in sepsis by modulating cell apoptosis. Mechanistically, RSAD2 knockdown significantly inhibited the activation of the NF-κB signaling pathway, resulting in the suppression of apoptosis. Taken together, our findings demonstrate for the first time that targeting RSAD2 may be a potential therapeutic approach for sepsis.

RSAD2 (viperin), an interferon-inducible protein with well-established antiviral functions, has recently emerged as a critical modulator of inflammatory responses. While its role in viral infections was well documented, our study provided novel insights into its previously underappreciated involvement in bacterial endotoxin signaling and sepsis-associated acute lung injury (ALI). Lipopolysaccharide (LPS), a component of the outer membrane of Gram-negative bacteria, has been shown to upregulate the expression of RSAD2 in various cell types significantly.

Through analysis of public databases, we found that the expression of RSAD2 in human alveolar macrophages was significantly increased after stimulation with LPS. Moreover, we also observed the same phenomenon in RAW264.7 cells. This finding, to some extent, corroborates the role of RSAD2 in sepsis-related ALI. As the core cells of lung immune regulation, alveolar macrophages (AMs) are very important for maintaining airway homeostasis and are involved in the development of various lung diseases.[18] The reduction in the number of alveolar macrophages due to apoptosis of alveolar macrophages reduces their ability to phagocytize inflammatory effector cells, leading to the programmed release of a large number of inflammatory mediators by inflammatory cells, thus exacerbating lung injury. Bioinformatics analyses (GO, KEGG, and GSEA) revealed that apoptosis pathways were significantly upregulated in LPS-stimulated alveolar macrophages. In sepsis-induced ALI, excessive apoptosis of alveolar macrophages can impair

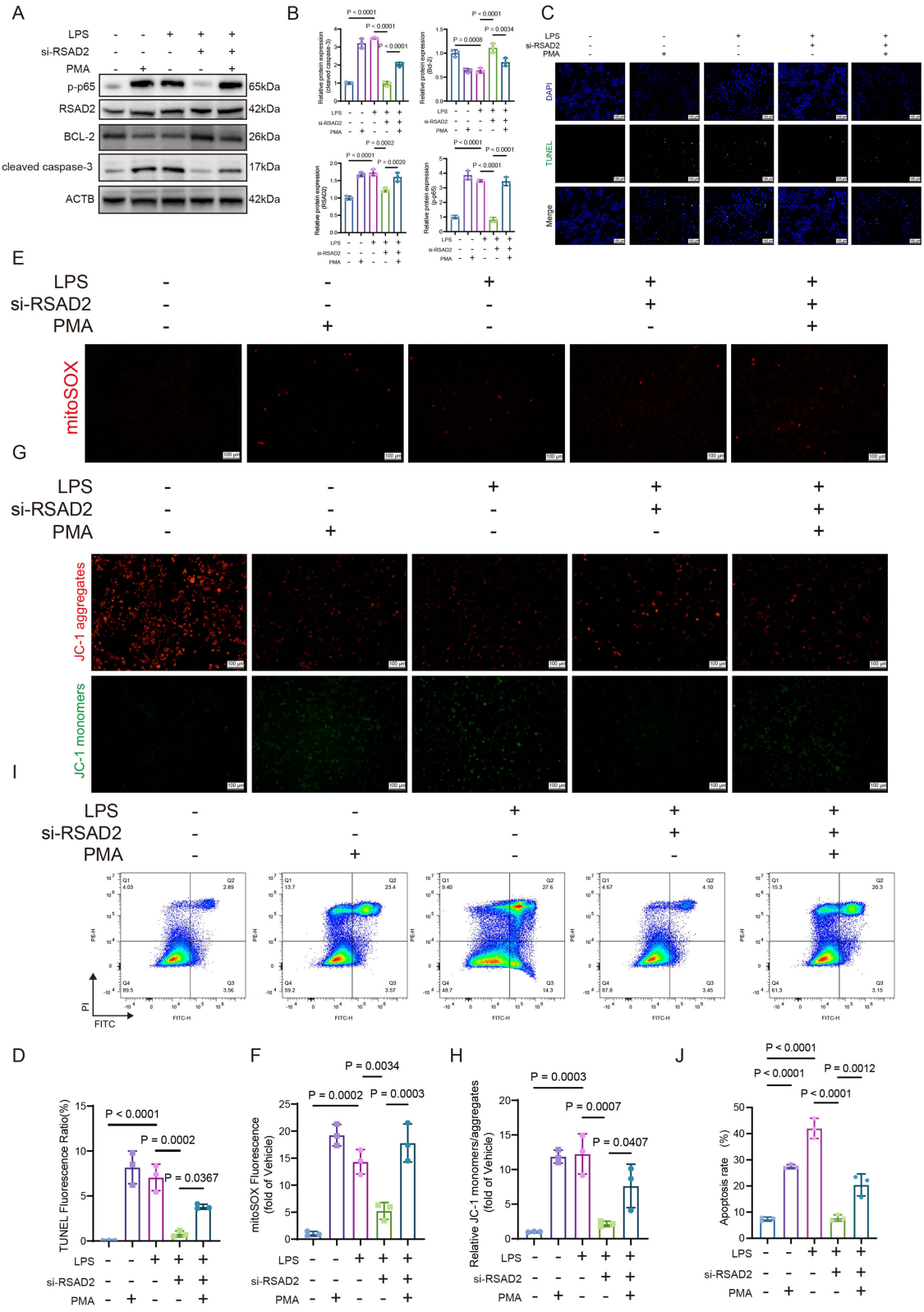


**Figure 6** PMA reversed the protective effect of RSAD2 knockdown on apoptosis in vitro. (**A** and **B**) Western blot results of p-p65, RSAD2, Bcl-2, and cleaved caspase-3 protein expression levels, n = 3. (**C**) TUNEL staining of cell apoptosis. (**D**) Quantification of TUNEL-positive cells, n=3. (**E** and **F**) MitoSOX staining and fluorescence intensity quantification of RAW264.7, n = 3. (**G**) Typical JC-1 staining patterns observed in LPS-stimulated RAW264.7 cells. (**H**) Fluorescence signal intensity was quantified, n = 3. (**I** and **J**) Flow cytometry analysis of apoptosis in vitro. Data with normal distribution are presented as mean ± SD.


https://doi.org/10.2147/JIR.S535225

their phagocytic ability, leading to increased inflammatory mediator release and exacerbated lung injury.[19,20] Western blot, TUNEL assays, and flow cytometry confirmed these findings in RAW264.7 cells. Meanwhile, using siRNA to knock down RSAD2 in RAW264.7 cells, we found that reducing RSAD2 expression attenuated LPS-induced macrophage apoptosis.

Previous studies have shown that NF-κB signaling plays a pivotal role in immune and inflammatory responses, with dysregulation linked to numerous diseases, including cancer, autoimmune disorders, and sepsis.[21] The NF-κB transcription factor family, comprising NF-κB1 (p105/p50), NF-κB2 (p100/p52), p65 (RELA), RELB, and c-REL, forms homo or heterodimers, with the p65/p50 dimer being the most common.[22] In LPS-stimulated macrophages, persistent nuclear accumulation of p65 drives NF-κB activation, creating a positive feedback loop that amplifies the inflammatory response.[23] NF-κB plays a dual role in apoptosis regulation, mediating a balance between survival and cell death. Studies have shown that macrophage polarization to the M1 phenotype can activate NF-κB and promote mitochondrial-mediated apoptosis.[24] Conversely, inhibiting NF-κB activation in certain cell types reduces apoptosis by modulating the expression of Bcl-2 and Bax.[25] Phosphorylation of p65, a hallmark of NF-κB activation, was used as a key indicator to assess pathway activity. We found that RSAD2 knockdown significantly inhibited the activation of the NF-κB pathway. These findings align with reports that RSAD2 knockdown in LPS-stimulated microglia reduces activation of the NF-κB pathway, suppressing proinflammatory factor expression and alleviating neuropathic pain.[26] Knockout of the S100A9 gene in macrophages can alleviate LPS-induced ALI by downregulating TLR4/MyD88/NF-κB signal conduction to regulate M1 macrophage polarization and inhibit pyroptosis.[20] Circ-Phkb induces alveolar macrophage apoptosis and increases inflammation by promoting TLR4/MyD88/NF-κB.[19] However, conflicting studies suggest that RSAD2 may also inhibit NF-κB activation under certain conditions, impairing innate immune responses.[27] In various cell types, RSAD2 consistently exerts its effects by activating the NF-κB pathway, such as promoting microglial activation[16] and inducing keratinocytes to secrete pro-inflammatory mediators.[15] However, a divergent response was observed in Mycobacterium tuberculosis-infected macrophages, likely attributable to infection-specific alterations. These discrepancies may result from variations in experimental conditions, cell types, and stimuli, highlighting the complexity of RSAD2's regulatory mechanisms on the NF-κB signaling pathway.

To further clarify whether RSAD2 attenuates the apoptosis of RAW264.7 cells via the NF-κB signaling pathway, PMA (NF-κB activator) was used. We found that the use of PMA significantly reversed the protective effect of RSAD2 knockdown against apoptosis in RAW264.7 cells. The findings revealed that RSAD2 exerts its anti-apoptotic effect against LPS through NF-κB pathway-mediated regulation of apoptosis-related proteins.

Despite these significant findings, our study has several limitations: 1) All experiments were conducted in vitro using RAW264.7 cells. Further, in vivo studies in animal models are needed to confirm the role of RSAD2 in ALI. 2) In our cell experiments, the results were replicated only three times, resulting in limited statistical power. However, our preliminary findings remain valid and warrant further verification in studies with larger sample sizes to enhance statistical robustness. 3) While we assessed NF-κB activation by measuring p65 phosphorylation, additional studies on downstream NF-κB targets and signaling pathways are necessary to fully elucidate the molecular mechanisms. 4) We only used the siRNA to knock down the expression of RSAD2. Targeting RSAD2 with selective inhibitors (eg, siRNA nanocarriers) could potentially attenuate sepsis-induced ALI by dual suppression of inflammation and cell death, offering a novel approach beyond current anticytokine therapies. 5) RSAD2 knockdown may alleviate sepsis-induced macrophage apoptosis via its anti-inflammatory action, though this contradicts its known antiviral function, indicating potential limitations for treating mixed infections.

## Conclusion

This study underscored the pivotal role of RSAD2 in sepsis. We demonstrated that RSAD2 knockdown mitigates macrophage apoptosis by suppressing NF-κB signaling, providing novel insights into RSAD2 as a potential therapeutic target for sepsis-related ALI and ARDS. Further research is needed to explore the translational potential of these findings in clinical applications.

## Ethics Approval and Informed Consent

This study is exempt from ethical review in accordance with item 1 of Article 32 of the Measures for Ethical Review of Life Science and Medical Research Involving Human Subjects dated February 18, 2023, China. The specific provision is as follows: Article 32: Ethical review may be exempted for human life science and medical research involving the use of personal information data or biological samples under the following circumstances, provided that the research causes no harm to human subjects and involves no sensitive personal information or commercial interests, so as to reduce unnecessary burdens on researchers and facilitate such studies: (1) Research utilizing legally obtained publicly available data or data generated through observation of public behavior without interference.

## Data Sharing Statement

The datasets generated and/or analysed during the current study are available in the [GENE EXPRESSION OMNIBUS (GEO) database] repository, [https://www.ncbi.nlm.nih.gov/gds/]. The datasets generated during and/or analysed during the current study are available from the corresponding author on reasonable request.

## Funding

This work was supported by the Fundamental Research Funds for the Central Universities of Central South University (Grant number: 2023ZZTS0208) and Hunan Provincial Innovation Foundation for Postgraduate (Grant number: CX20230284).

## Disclosure

The authors declare that there are no conflicts of interest.

## References

1. Feng L, Song P, Zhou H. et al. Pentamethoxyflavanone regulates macrophage polarization and ameliorates sepsis in mice. *Biochem Pharmacol*. 2014;89(1):109–118. doi:10.1016/j.bcp.2014.02.016
2. Liu F, Peng W, Chen J, et al. Exosomes Derived From Alveolar Epithelial Cells Promote Alveolar Macrophage Activation Mediated by miR-92a-3p in Sepsis-Induced Acute Lung Injury. *Front Cell Infect Microbiol*. 2021;11:646546. doi:10.3389/fcimb.2021.646546
3. Khan MM, Yang W-L, Wang P. ENDOPLASMIC RETICULUM STRESS IN SEPSIS. *Shock*. 2015;44(4):294–304. doi:10.1097/SHK.0000000000000425
4. Gordon S, Martinez-Pomares L. Physiological roles of macrophages. *Pflugers Arch - Eur J Physiol*. 2017;469(3–4):365–374. doi:10.1007/s00424-017-1945-7
5. Nepal S, Tiruppathi C, Tsukasaki Y, et al. STAT6 induces expression of Gas6 in macrophages to clear apoptotic neutrophils and resolve inflammation. *Proc Natl Acad Sci USA*. 2019;116(33):16513–16518. doi:10.1073/pnas.1821601116
6. Chen X, Liu Y, Gao Y, Shou S, Chai Y. The roles of macrophage polarization in the host immune response to sepsis. *Int Immunopharmacol*. 2021;96:107791. doi:10.1016/j.intimp.2021.107791
7. Bosca L, Zeini M, Traves P, Hortelano S. Nitric oxide and cell viability in inflammatory cells: a role for NO in macrophage function and fate. *Toxicology*. 2005;208(2):249–258. doi:10.1016/j.tox.2004.11.035
8. Jena S, Ray A, Mohanta O, et al. Neocinnamomum caudatum Essential Oil Ameliorates Lipopolysaccharide-Induced Inflammation and Oxidative Stress in RAW 264.7 Cells by Inhibiting NF-κB Activation and ROS Production. *Molecules*. 2022;27(23):8193. doi:10.3390/molecules27238193
9. Wesche-Soldato D, Swan R, Chung C-S, Ayala A. The Apoptotic Pathway as a Therapeutic Target in Sepsis. *CDT*. 2007;8(4):493–500. doi:10.2174/138945007780362764
10. Lai K, Song C, Gao M, et al. Uridine Alleviates Sepsis-Induced Acute Lung Injury by Inhibiting Ferroptosis of Macrophage. *IJMS*. 2023;24(6):5093. doi:10.3390/ijms24065093
11. Pan X, He L. LncRNA MEG3 expression in sepsis and its effect on LPS-induced macrophage function. *Cell Mol Biol*. 2020;66(5):131–136. doi:10.14715/cmb/2020.66.5.23
12. Zhu H, Cong J-P, Shenk T. Use of differential display analysis to assess the effect of human cytomegalovirus infection on the accumulation of cellular RNAs: induction of interferon-responsive RNAs. *Proc Natl Acad Sci USA*. 1997;94(25):13985–13990. doi:10.1073/pnas.94.25.13985
13. Rivera-Serrano EE, Gizzi AS, Arnold JJ, Grove TL, Almo SC, Cameron CE. Viperin Reveals Its True Function. *Annu Rev Virol*. 2020;7(1):421–446. doi:10.1146/annurev-virology-011720-095930
14. Weinstein AG, Godet I, Gilkes DM. The rise of viperin: the emerging role of viperin in cancer progression. *J Clin Investig*. 2022;132(24):e165907. doi:10.1172/JCI165907
15. Li X, Chen F, Li Y, et al. Downregulation of RSAD2 ameliorates keratinocyte hyperproliferation and skin inflammation in psoriasis via the TAK1/NF-κB axis. *Biochem Pharmacol*. 2025;233:116764. doi:10.1016/j.bcp.2025.116764
16. Gao X, Gao L, Zhang Y, Kong X, Jia S, Meng C. Huc-MSCs-derived exosomes attenuate neuropathic pain by inhibiting activation of the TLR2/MyD88/NF-κB signaling pathway in the spinal microglia by targeting Rsad2. *Int Immunopharmacol*. 2023;114:109505. doi:10.1016/j.intimp.2022.109505

17. Li P, Hao Z, Wu J, et al. Comparative Proteomic Analysis of Polarized Human THP-1 and Mouse RAW264.7 Macrophages. *Front Immunol*. 2021;12:700009. doi:10.3389/fimmu.2021.700009
18. Hussell T, Bell TJ. Alveolar macrophages: plasticity in a tissue-specific context. *Nat Rev Immunol*. 2014;14(2):81–93. doi:10.1038/nri3600
19. Wei X, Yi X, Liu J, et al. Circ-phkb promotes cell apoptosis and inflammation in LPS-induced alveolar macrophages via the TLR4/MyD88/NF-kB/CCL2 axis. *Respir Res*. 2024;25(1):62. doi:10.1186/s12931-024-02677-6
20. Gong C, Ma J, Deng Y, et al. S100A9-/- alleviates LPS-induced acute lung injury by regulating M1 macrophage polarization and inhibiting pyroptosis via the TLR4/MyD88/NFκB signaling axis. *Biomed Pharmacother*. 2024;172:116233. doi:10.1016/j.biopha.2024.116233
21. Capece D, Verzella D, Flati I, Arboretto P, Cornice J, Franzoso G. NF-κB: blending metabolism, immunity, and inflammation. *Trends Immunol*. 2022;43(9):757–775. doi:10.1016/j.it.2022.07.004
22. Guo Q, Jin Y, Chen X, et al. NF-κB in biology and targeted therapy: new insights and translational implications. *Signal Transduction and Targeted Therapy*. 2024;9:53.
23. Sung M-H, Li N, Lao Q, Gottschalk RA, Hager GL, Fraser IDC. Switching of the Relative Dominance Between Feedback Mechanisms in Lipopolysaccharide-Induced NF-κB Signaling. *Sci Signal*. 2014;7:ra6.
24. Huang Y-L, Zhang F-L, Tang X-L, Yang X-J. Telocytes Enhances M1 Differentiation and Phagocytosis While Inhibits Mitochondria-Mediated Apoptosis Via Activation of NF-κB in Macrophages. *Cell Transplant*. 2021;30:096368972110027. doi:10.1177/09636897211002762
25. Li X. Mir-199a-5p regulates the proliferation and apoptosis of degenerative nucleus pulposus cells through the cdkn1b/nf-κb axis. *Shock*. 2022;58(5):384–392. doi:10.1097/SHK.0000000000002002
26. Jang J-S, Lee J-H, Jung N-C, et al. Rsad2 is necessary for mouse dendritic cell maturation via the IRF7-mediated signaling pathway. *Cell Death Dis*. 2018;9(8):823. doi:10.1038/s41419-018-0889-y
27. Zhou X, Zhang Z, Xu H, et al. Viperin impairs the innate immune response through the IRAK1-TRAF6-TAK1 axis to promote Mtb infection. *Sci Signal*. 2022;15(754):eabe1621. doi:10.1126/scisignal.abe1621